Experimental Cell Research 405 (2021) 112684

Contents lists available at ScienceDirect

Experimental Cell Research

journal homepage: www.elsevier.com/locate/yexcr

CTPS forms the cytoophidium in zebrafish

Chia-Chun Chang [a,1], Gerson Dierley Keppeke [a,c,1], Christopher L. Antos [a], Min Peng [b], Luis Eduardo Coelho Andrade [c], Li-Ying Sung [b,d], Ji-Long Liu [a,e,*]

[a] School of Life Science and Technology, ShanghaiTech University, Shanghai, 201210, China
[b] Institute of Biotechnology, National Taiwan University, Taipei, 106, Taiwan
[c] Rheumatology Division, Escola Paulista de Medicina, Universidade Federal de Sao Paulo, Sao Paulo, SP 04023-062, Brazil
[d] Agricultural Biotechnology Research Center, Academia Sinica, Taipei, 115, Taiwan
[e] Department of Physiology, Anatomy and Genetics, University of Oxford, Oxford, OX1 3PT, United Kingdom

ARTICLE INFO

Keywords:
CTPS
Cytoophidium
Zebrafish

ABSTRACT

Cytidine triphosphate synthase (CTPS) catalyzes the rate-limiting step of de novo CTP biosynthesis. An intracellular structure of CTPS, the cytoophidium, has been found in many organisms including prokaryotes and eukaryotes. Formation of the cytoophidium has been suggested to regulate the activity and stability of CTPS and may participate in certain physiological events. Herein, we demonstrate that both CTPS1a and CTPS1b in zebrafish are able to form the cytoophidium in cultured cells. A point mutation, H355A, abrogates cytoophidium assembly of zebrafish CTPS1a and CTPS1b. In addition, we show the presence of CTPS cytoophidia in multiple tissues of larval and adult fish under normal conditions, while treatment with a CTPS inhibitor 6-diazo-5-oxo-L-norleucine (DON) can induce more cytoophidia in some tissues. Our findings reveal that forming the CTPS cytoophidium is a natural phenomenon of zebrafish and provide valuable information for future research on the physiological importance of this intracellular structure in vertebrates.

1. Introduction

Several metabolic enzymes have been reported as able to assemble into filamentous macrostructures, termed cytoophidia ('cellular snakes' in Greek), in numerous organisms. These microscale structures are proposed to fine-tune various protein properties [1,2]. Cytidine triphosphate synthase (CTPS) and inosine 5′-monophosphate dehydrogenase (IMPDH) are two of the best known cytoophidium-forming proteins. More recently, a number of metabolic enzymes have joined the list with detailed characterization, such as phosphoribosyl pyrophosphate synthetase 1 (PRPS1), asparagine synthetase (ASNS) and delta-1-pyrroline-5-carboxylate synthase (P5CS), among others [3–5]. With an accumulation of evidence, polymerization and forming larger aggregates are believed to represent a common mechanism for many enzymes.

CTPS catalyzes the final and rate-limiting step of the de novo CTP synthetic pathway, in which UTP is converted into CTP with the consumption of ATP and glutamine. CTPS contains binding sites for ATP, UTP, CTP and GTP. While ATP and UTP serve as substrates, GTP is required for utilizing glutamine and CTP negatively regulates its activity. In the presence of the substrates, CTPS will be found in a tetrameric state, its active form. CTPS tetramers can further pile up to form polymers, which are the subunits of the cytoophidium structure in the cell [6,7]. A residue His 355 of human CTPS (hCTPS), which sits at the interface of two neighboring tetramers within the polymer, plays a critical role in CTPS polymerization. Mutations such as H355A abrogating this interaction also prevent cytoophidium formation in the cell [7]. Recent structural and biochemical analysis indicates that polymerization of hCTPS desensitizes the inhibitory effect of CTP, thereby enhancing CTP production [7,8]. Yet, an opposite effect was observed on *Escherichia coli* CTPS as increasing the level of polymerization reduced the catalytic activity [9]. These contradictory findings imply that the functions of the cytoophidium may differ among species.

The CTPS cytoophidium has been found in organisms across most kingdoms of life: from unicellular organisms such as archaea, bacteria and yeast to insects, plants and mammals [6,10–15]. In unicellular models, depending on the organism, the CTPS cytoophidium is likely to appear at specific phases of growth, and is also strongly influenced by

* Corresponding author. School of Life Science and Technology, ShanghaiTech University, Shanghai, 201210, China.
E-mail addresses: jilong.liu@dpag.ox.ac.uk, liujl3@shanghaitech.edu.cn (J.-L. Liu).
[1] These authors contributed equally to this work.

https://doi.org/10.1016/j.yexcr.2021.112684
Received 21 March 2021; Received in revised form 30 May 2021; Accepted 1 June 2021
Available online 12 June 2021

changes in the environment [6,11,12,15–17,39]. In mammalian cultured cells, CTPS cytoophidium formation can be induced by deprivation of glutamine or treatment with CTPS inhibitors, such as 6-diazo-5-oxo-L-norleucine (DON) and deazauridine (DAU) [18–20]. In fruit flies, CTPS cytoophidia were found in many tissues, including brain, gut, trachea, testis, salivary gland and egg chambers under normal physiological conditions [10]. The localization of the cytoophidium could be determined by cell polarity, suggesting its association with other cellular compartments in some cell types [40]. In human tissues, cytoophidia have been observed in various cancerous and non-cancerous samples, implying a correlation with tissue-specific metabolism [21]. In fact, formation of the CTPS cytoophidium has been demonstrated to positively correlate with c-Myc expression and the mTOR-S6K1 pathway [22–24].

Due to the lack of mutant animal models with a 'no-cytoophidium' phenotype, the physiological importance of the CTPS cytoophidium has not been analyzed *in vivo* in multicellular organisms. Considering the advantages of using zebrafish (*Danio rerio*) as a vertebrate model animal for genetic study, we aimed to investigate the cytoophidium-forming properties of zebrafish CTPS (zfCTPS). Herein, we show that both zfCTPS1a and zfCTPS1b are able to assemble the cytoophidium when expressed in a human cell line. The effect of a H355A point mutation is conserved between hCTPS and zfCTPS, implying a similarity in polymeric structures. In larval and adult fish we observed the presence of CTPS cytoophidia in various tissues under normal physiological conditions. Treatment with DON stimulated more cytoophidia in gallbladder and gut of lavae. Our findings demonstrate that the zfCTPS cytoophidium may play a role during fish development and is associated with certain functions of specific tissues. The characteristics shared by zfCTPS and mammalian CTPS reinforce zebrafish as a promising model animal for CTPS cytoophidium research.

2. Results and discussion

2.1. *zfCTPS1a and zfCTPS1b are capable of forming cytoophidia in human cells*

There are two CTPS isoforms, zfCTPS1a and zfCTPS1b, encoded by different genes in the zebrafish genome. Both isoforms share 86% sequence similarity to hCTPS1 and around 75% sequence similarity to hCTPS2 (Fig. 1A). Despite an identical function, hCTPS1 and hCTPS2 may have distinct expression patterns throughout the body. Generally, hCTPS1 is the predominant isoform in human tissues and plays a critical role in lymphocyte proliferation [25]. In zebrafish, morpholino-based knockdown of zfCTPS1a, but not zfCTPS1b, during early development induces more severe, long-lasting defects [26]. Thus, we first aimed to determine expression levels of zfCTPS1a and zfCTPS1b in various tissues of adult animals and 10 dpf (days post fertilization) larvae by RT-qPCR. While zfCTPS1a showed the highest expression level in a mixture of organs of adult fish, zfCTPS1b showed higher levels in adult eyes and larval fish (Fig. 1B), suggesting differences in preferential expression of CTPS isoforms among developmental stages and organs.

Next, we aimed to investigate the cytoophidium-forming properties of the two zfCTPS isoforms. To this end, we cloned the coding sequences of both zfCTPS1a and 1b into vectors with flag-tag and myc-tag at N-terminus, respectively. Constructs were then delivered into HEK 293T cells for transient expression. One *anti*-hCTPS1 polyclonal antibody was used in immunofluorescence on transfected cells for validating its specificity. In the cells expressing higher amounts of zfCTPS1a protein, which are indicated by strong labeling of *anti*-flag antibody, a stronger signal of *anti*-hCTPS1 antibody was also observed (Fig. 2A). However, cells with high zfCTPS1b expression showed no increase in the intensity of *anti*-hCTPS1 antibody signal, indicating that the antibody has high affinity to zfCTPS1a but not zfCTPS1b (Fig. 2A).

The CTPS cytoophidium is known to be a large bundle of CTPS filaments and possibly differs greatly in sizes depending on the amount of proteins incorporated into the structure. Without further treatments, we noticed unusual structures outlined by antibodies against tags in

A

Sequence Identity (%)			
	zfCTPS1a	zfCTPS1b	hCTPS1
zfCTPS1b	89		
hCTPS1	86.63	86.13	
hCTPS2	75.47	74.19	74.28

B

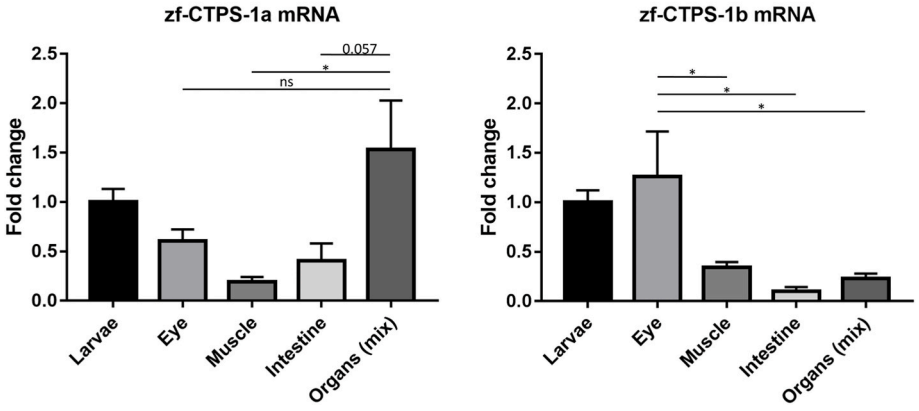

Fig. 1. Differential expression patterns of zebrafish CTPS1a and CTPS1b. (A) Comparison of sequence identity between zfCTPS and human CTPS isoforms. (B) Bar graphs showing relative mRNA levels of zfCTPS isoforms in different organs of adult fish (n = 4) and larval fish (10 dpf). Larva ΔCt average was considered as 1 for the comparison using the ΔΔCt method (see RT-qPCR methods for details). The larva ΔCt average of zfCTPS1a is 0.230 (SD ± 0.042) and of zfCTPS1b is 0.266 (SD ± 0.046). Error bars = SEM. *p < 0.05.

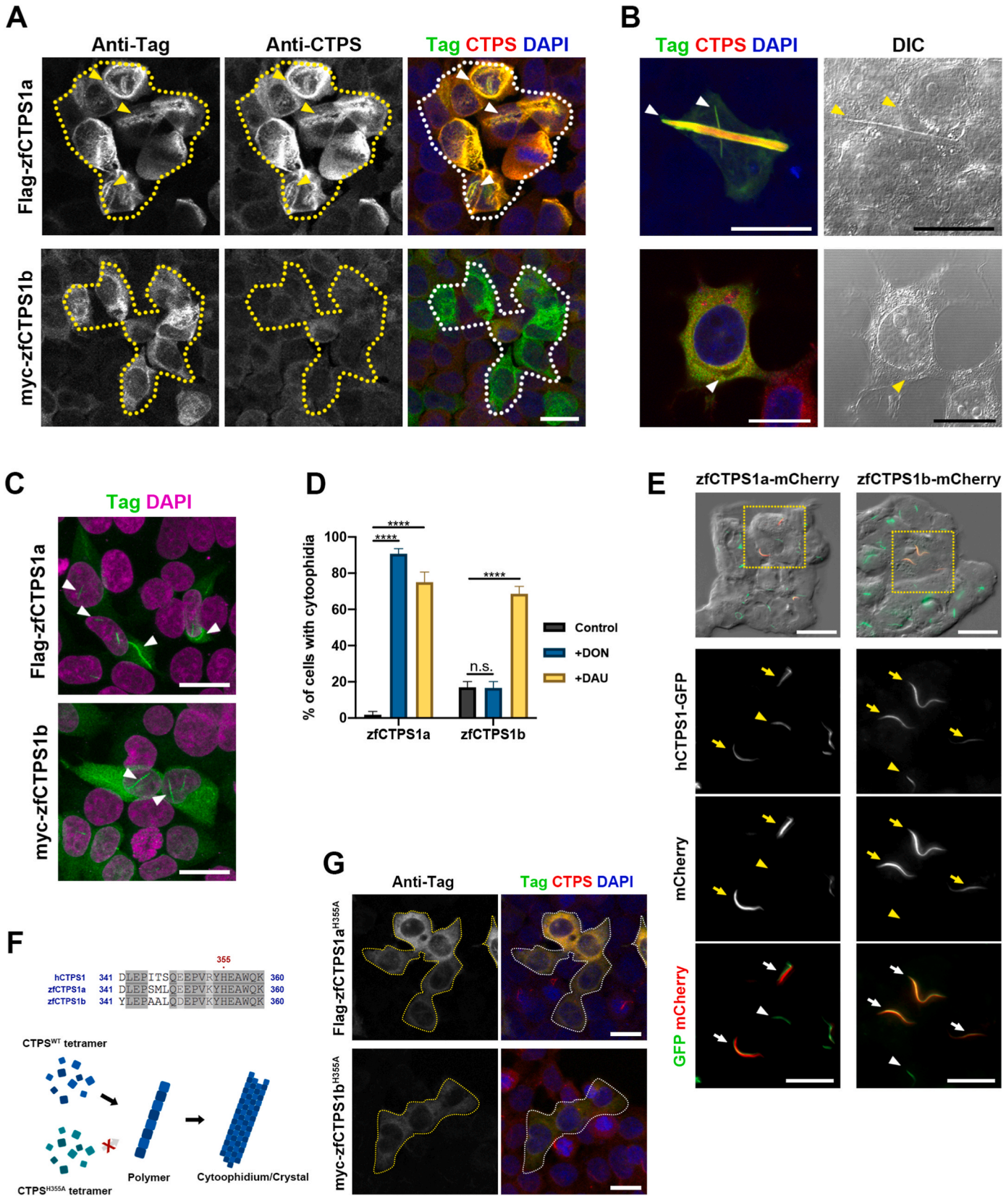

(caption on next page)

Fig. 2. zfCTPS polymers can form cytoophidia and crystals in HEK 293T cells. (A) Immunofluorescence of HEK 293T cells expressing zfCTPS isoforms. Cells with strong labeling for Flag-tag or Myc-tag are outlined. *In cellulo* crystals are indicated by arrowheads. (B) Immunofluorescent images and correspondent DIC images of representative cells with zfCTPS1a and zfCTPS1b crystals. (C) Immunofluorescence of Flag-zfCTPS1a and Myc-zfCTPS1b expressing HEK 293T cells treated with DAU (100 μM) for 5 h. The zfCTPS cytoophidia are indicated by arrowheads. (D) The bar graph shows the quantitative results of the proportion of transfected HEK 293T cells with zfCTPS1a or zfCTPS1b cytoophidia. Cells were treated with DON (10 μg/ml) or DAU (100 μM) for 5 h before fixation. At least 100 cells were counted in each group. Error bars = SEM. (****p value < 0.001, Student's t-test) (E) Fluorescent live-cell images of hCTPS1-GFP HEK 293T cells transfected with zfCTPS1a-mCherry or zfCTPS1b-mCherry. Cells were pretreated with DAU (100 μM) for 3 h before observation. Cytoophidia with GFP-hCTPS1 alone are indicated by arrowheads, while zfCTPS-mCherry and GFP-hCTPS1 mixed cytoophidia are indicated by arrows. (F) Sequence comparison of hCTPS1 and zfCTPS1a and zfCTPS1b at the H355 region and illustration of how the cytoophidium/crystal of zfCTPS is formed by polymers. (G) Immunofluorescent images of HEK 293T cells expressing H355A mutant zfCTPS isoforms. Transfected cells are outlined. Cells were treated with DON (10 μg/ml) for 1 day before fixation. No CTPS cytoophidia were observed in transfected cells, while some cytoophidia could be found in non-transfected cells. Scale bars = 20 μm in all panels.

zfCTPS1a and zfCTPS1b expressing cells (Figs. 2A and 3). In some cases, such structures can be observed in differential interference contrast (DIC) images (Fig. 2B). In our previous studies, large cytoophidia were frequently found in CTPS-overexpressing cells under specific conditions [18]. However, even the cytoophidia in large sizes could not be observed without the label of antibodies. Herein, the structures in zfCTPS overexpressing cells were frequently labeled by antibodies in partial and could be observed directly through DIC microscope, suggesting it is a more compact structure than typical cytoophidia. Therefore, we speculate that these structures are "*in cellulo* crystals" of zfCTPS. Indeed, increasing evidence has highlighted that recombinant proteins can form intracellular crystals in host cells [27,28]. The proportion of cells with zfCTPS crystals is related to the expression levels of zfCTPS1a and zfCTPS1b, as much fewer cells with crystals were observed when less amount of DNA was used for transfection (Fig. 3).

High CTPS overexpression in mammalian cells does not trigger cytoophidium assembly, but such cells more frequently display large cytoophidia when treated with CTPS inhibitors [29]. To examine whether zfCTPS1a and zfCTPS1b can assemble the cytoophidium in host cells, we treated transfected HEK 293T cells with DON or DAU for 5 hours. DON and DAU treatments effectively induced zfCTPS1a cytoophidia in about 90% and 75% of transfected cells, respectively (Fig. 2C and D). Meanwhile, zfCTPS1b cytoophidia, were observed in about 17% of transfected cells without additional stimulus, and in 69% of cells treated with DAU. The treatment of DON failed to induce more zfCTPS1b cytoophidia, suggesting distinct filament forming properties of two zfCTPS isoforms. We also constructed zfCTPS1a-mCherry and zfCTPS1b-mCherry fluorescent fusion proteins and expressed them in a HEK 293T cell line with GFP tagging endogenous hCTPS1 protein. With this combination, we were able to trace the localization of hCTPS1-GFP and zfCTPS-mCherry in live cells. Upon treatment with DAU for 3 hours, cytoophidia labeled by GFP and mCherry were clearly seen in the cells

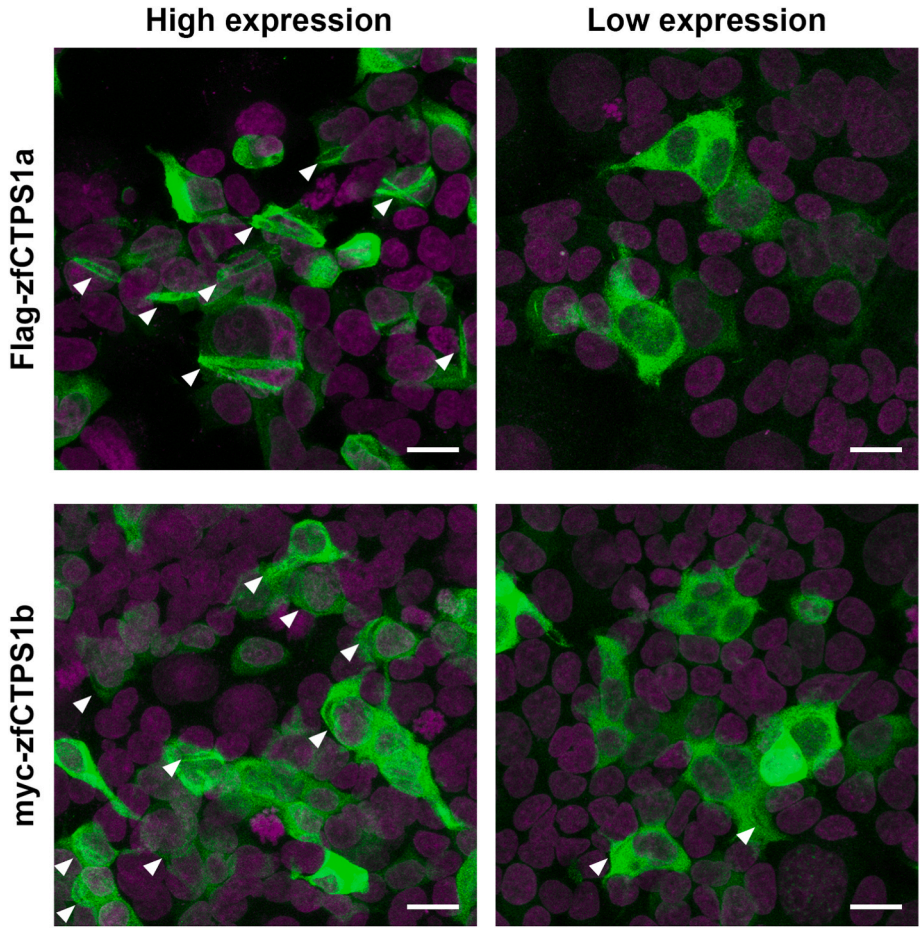

Fig. 3. Formation of zfCTPS crystals is correlated with expression levels. Immunofluorescence of HEK 293T cells expressing zfCTPS isoforms. Cells cultured in the 24-well plate were transfected with plasmid in high or low quantity (500 ng or 100 ng per well) and fixed one day after transfection. Antibodies against Flag-tag or Myc-tag are shown in green and DAPI is shown in magenta. *In cellulo* crystals are indicated by arrowheads. Scale bars = 20 μm.

(Fig. 2E). Interestingly, in the transfected cells GFP-labeled and mCherry-labeled cytoophidia seemed to colocalize. However, with a closer look, it could be seen that zfCTPS and hCTPS cytoophidia were actually separate structures (Fig. 2E), and so this is similar to the interaction between CTPS and IMPDH cytoophidia described previously (Chang et al. 2018a). These findings indicate that both zfCTPS1a and zfCTPS1b are capable of assembling the cytoophidium in human cells.

A previous structural study on hCTPS1 revealed that a critical point mutation, H355A, can abrogate hCTPS1 polymerization without interfering with tetramerization [7]. Since sequences of hCTPS1 and zfCTPS are conserved at this region, we wondered whether a H355A mutation on zfCTPS would also prevent cytoophidium formation (Fig. 2F). We transfected HEK 293T cells with constructs encoding H355A mutant zfCTPS1 isoforms and performed immunofluorescence on cells treated with DON for 1 day. As the result, none of the cells with mutant zfCTPS1a and zfCTPS1b expression showed cytoophidia, not even the ones formed by endogenous hCTPS, suggesting that mutant zfCTPS may interfere with the aggregation of hCTPS (Fig. 2G). Moreover, the *in cellulo* crystals of zfCTPS were not observed in these cells under conditions either with or without DON, suggesting that the cytoophidium and the crystal structure are both composed of zfCTPS polymers.

2.2. *zfCTPS forms the cytoophidium in fish larva*

In the previous experiments we showed that the *anti*-hCTPS1 antibody can label zfCTPS1a. We then wanted to examine whether zfCTPS assembles the cytoophidium *in vivo* during embryo development. We performed whole-mount immunofluorescence on embryos from 2 to 9 hpf (hours post fertilization) and larval fish at the age of 5 and 8 dpf. In the embryos there were no detectable CTPS cytoophidia (data not shown). In the larval fish, cytoophidia were observed in the pronephric duct (cloaca region) and in the branchia of some 5 and 8 dpf specimens (Fig. 4). In the cloaca region, cytoophidia were seen in 21% and 85% of 5 and 8 dpf larvae, respectively. Meanwhile, 36% and 62% of 5 and 8 dpf larvae had cytoophidia in the branchia. (Fig. 4F). We also calculated the proportion of cells presenting cytoophidia in the cloaca region of the pronephric duct, and found this to be about 23% in both 5 and 8 dpf larvae. In the branchia, we quantified the number of detectable

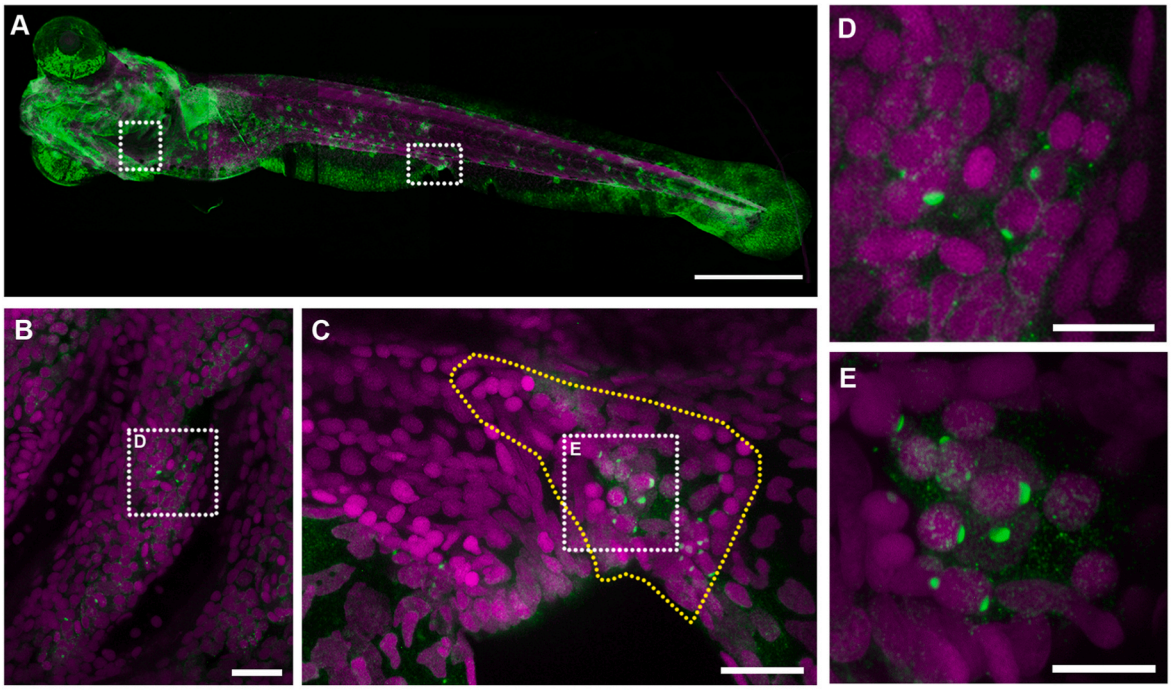

F

Specimens		
Day 5-Larvae (n=14)	**Cytoophidium in pronephric duct (cloaca)**	21% (3)
	Proportion of cells with cytoophidia	23% (±1.9%)
	Cytoophidium found in branchia	36% (5)
	Average number of cytoophidium	17 (±15.8)
Day 8-Larvae (n=13)	**Cytoophidium in pronephric duct (cloaca)**	85% (11)
	Proportion of cells with cytoophidia	23% (±13%)
	Cytoophidium found in branchia	62% (8)
	Average number of cytoophidium	26 (±15.4)

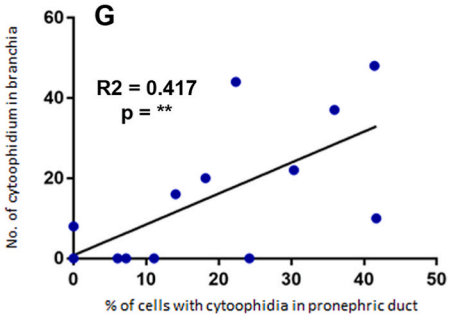

Fig. 4. zfCTPS forms the cytoophidium in zebrafish larvae. (A) Whole-mount immunofluorescence of 8 dpf larvae with the *anti*-hCTPS1 antibody (shown in green). Hoechst is shown in magenta. Cytoophidia were observed in the branchia (B) and cloaca region of pronephric duct (C, highlighted by yellow dash line). (D and E) Magnified view of selected areas in (B) and (C), respectively. (F) Quantification of the number of cytoophidia observed in the branchia and the proportion of cells with cytoophidia in the cloaca region of pronephric duct in 5 and 8 dpf larvae. (G) In 8 dpf larvae (n = 13), a positive correlation was observed between the number of cytoophidia in branchia and the proportion of cells with the cytoophidium in cloaca (Pearson $R^2 = 0.417$; **p = 0.01). Scale bars = 500 μm in (A), 20 μm in (B and C) and 10 μm in (D and E).

cytoophidia, and found 26 in each 8 dpf larva, on average (Fig. 4F). Furthermore, in all the 8 dpf larval fish samples (n = 13), there was a significant correlation between the number of cytoophidia in the branchia and the proportion of cytoophidium-presenting cells in the cloaca region, with $R^2 = 0.417$ ($p < 0.01$) (Fig. 4G), suggesting that CTPS cytoophidium regulation correlates with the metabolic state of the whole fish.

2.3. *zfCTPS forms the cytoophidium in multiple organs of adult fish*

To further explore the CTPS cytoophidium in adult fish, we performed immunofluorescence on cryosections of adult fish (n = 4) with the same *anti*-hCTPS1 antibody. Tissues and organs were identified by morphology, referring to previous reports [30]. Many cytoophidia were observed in the secondary lamella of the gills in all specimens, with a curious pattern (Fig. 5A–D). In these cells, the nucleus is surrounded by multiple cytoophidia. We quantified the number of cytoophidia in 100 randomly selected cytoophidium-presenting cells of the gills, and found an average of 5.4 (SD ± 1.3) cytoophidia per cell (arrows in Fig. 5C and D).

In the ovary, many cytoophidia were observed in the pre-vitellogenic and vitellogenic follicles (Fig. 5E–G). In the pre-vitellogenic follicles, cytoophidia are distributed within the oocyte cytoplasm, while in the vitellogenic follicles they are mostly located at the region near the *zona radiata* of the oocytes (arrows in Fig. 5F and G). We also examined eye tissues, where cytoophidia were distributed in the stroma layer of the cornea, but not in the retina (Fig. 5H and Fig. 6G).

In summary, in the adult fish under normal physiological conditions, the CTPS cytoophidium can be observed in the secondary lamella of the gills, in the oocytes and in the cornea. In some other organs, including the intestine, liver, olfactory organ, cerebellum, muscle and skin, however, we found no evidence of the presence of cytoophidia (Fig. 6).

2.4. *DON induces CTPS cytoophidium formation in vivo*

The glutamine analog DON, is a well-known inducer of CTPS cytoophidium assembly. In various model organisms, such as fission yeast, fruit fly and mammalian cells, treatment with DON increases the number of detectable cytoophidia and also increases the length of cytoophidia [10,31,32]. Therefore, DON has been widely applied to study the characteristics and dynamics of the cytoophidium. Yet, in prokaryotes, DON shows an opposite effect on CTPS filaments [6].

To determine whether DON could effectively induce CTPS cytoophidia in zebrafish, we treated 7 dpf fish larvae with 10 μg/ml DON for 1 day before fixation. The larval fish did not have a higher death rate than under normal culture conditions, and showed no apparent abnormality in appearance either. By using whole-mount immunofluorescence, diverse patterns of CTPS cytoophidia were seen. In most cases, we saw no difference compared to fish without DON treatment. In about 30% of samples (7 of 24 fish), more CTPS cytoophidia were detected with long filament morphology in the gallbladder or gut (Fig. 7). Taken together, our results indicate that DON can promote CTPS cytoophidium assembly in zebrafish.

2.5. *Zebrafish as a model for cytoophidium study*

In the last decade, a type of macrostructure of metabolic enzymes, the cytoophidium, has emerged as a novel regulatory system for a number of metabolic processes [1,2]. The CTPS cytoophidium is evolutionally conserved as it has been found in organisms across the biological kingdoms. Yet, detailed studies have demonstrated that the functions and regulation of the CTPS cytoophidium may differ between species. For instance, independent structural and biochemical analysis of human, *Drosophila* and *E. coli* CTPS showed that CTPS polymerization facilitates CTP production in humans and *Drosophila* by desensitizing the inhibitory effect of CTP binding, while *E. coli* CTPS polymers display reduced catalytic activity [7–9,33]. On the other hand, the CTPS cytoophidium can be observed in many tissues of the fruit fly under physiological conditions, but is generally rare in normal human tissues [10,21]. These differences prompted us to investigate the presence and properties of the CTPS cytoophidium in zebrafish. This is a unique vertebrate animal model, particularly attractive for developmental biology and genome editing. For determining the physiological importance of the cytoophidium *in vivo*, a no-cytoophidium mutant model animal would be especially valuable.

Molecular drugs, such as glutamine analogs, azaserine and DON, and the uridine analog, DAU, can induce CTPS cytoophidium assembly in fruit flies and human cells [19,31]. However, treatment with DON disassembles the cytoophidium in bacteria [6]. These contradictory results may be attributed to the structural and regulatory diversities of CTPS among these species. In this zebrafish study, we firstly demonstrate that both zfCTPS1a and zfCTPS1b are able to form cytoophidium structures, and treatment with DON or DAU can induce zfCTPS cytoophidium formation. The H355A mutation on zfCTPS, which was proposed to prevent CTPS polymerization, impairs the ability to assemble large aggregates in cells. In fact, analysis of point mutations that interfere with CTPS polymerization has been carried out in human, *Drosophila* and *E. coli* cells on a structural basis. Since human and *Drosophila* CTPS show high similarity in their polymer structures, the same residue His 355, which is located at the helix region of the glutaminase domain, plays a critical role in the tetramer-tetramer interaction of both CTPS polymers. The mutation H355A has been reported to disturb the polymerization [7,33]. By contrast, the *E. coli* CTPS polymer, which is also built up from tetramers, has different interaction points between neighboring tetramers at their linker regions between two major domains of CTPS. Point mutations such as E277R, F281R, N285D and E289R, which impair this interaction, also prevent *E. coli* CTPS polymerization [9]. In summary, our findings provide evidence suggesting a high structural similarity between human and zebrafish CTPS. Additionally, the H355A point mutation could be applied in genome editing for the generation of a no-cytoophidium zebrafish mutant model.

The rabbit polyclonal *anti*-hCTPS1 antibody we used in this study showed much higher affinity for zfCTPS1a than zfCTPS1b, although the two isoforms are highly similar in sequence. Despite this intriguing specificity, we cannot rule out the possibility that zfCTPS1a and zfCTPS1b form the cytoophidium together, since colocalization of different CTPS isoforms in the same cytoophidium has been described for yeast and human cells [11,18].

The CTPS cytoophidium structure has been shown not only to enhance CTP production but also prolong the half-life of CTPS proteins in human cells [7,34]. These functions may facilitate nucleotide synthesis and benefit cell metabolism, especially for cell types that have a higher demand for nucleotides. Meanwhile, the active mTORC pathway is positively correlated with the regulation of CTPS cytoophidium formation in human and fission yeast cells [23,24]. By using immunofluorescence on whole-mount larval samples and cryosections of adult specimens, we identified the CTPS cytoophidium in various organs of the zebrafish. From our observations, cytoophidia are most abundant in the branchia and ovarian tissues of adult fish, in addition to the branchia and cloaca region at the end of the pronephric duct in larvae. However, special attention should be given to the cytoophidium in the fish respiratory system. Until 7 dpf, larvae rely predominantly, if not exclusively, on cutaneous respiration [35]. From 8 to 10 dpf, O_2-sensitive cells in the gills take over the role of respiration. The cytoophidium seems to appear initially in the branchia of 8 dpf larvae and continues to be present until adulthood. Additionally, in the adult animals, the abundant cytoophidia we found in the secondary lamella of the gills, where the cells responsible for O_2 uptake are located, present a distinctive distribution: >5 structures per *cell* localizing around the nucleus.

This is the first study to screen for the CTPS cytoophidium in a vertebrate animal under physiological conditions, and to determine tissues that present the cytoophidium and may serve as suitable models

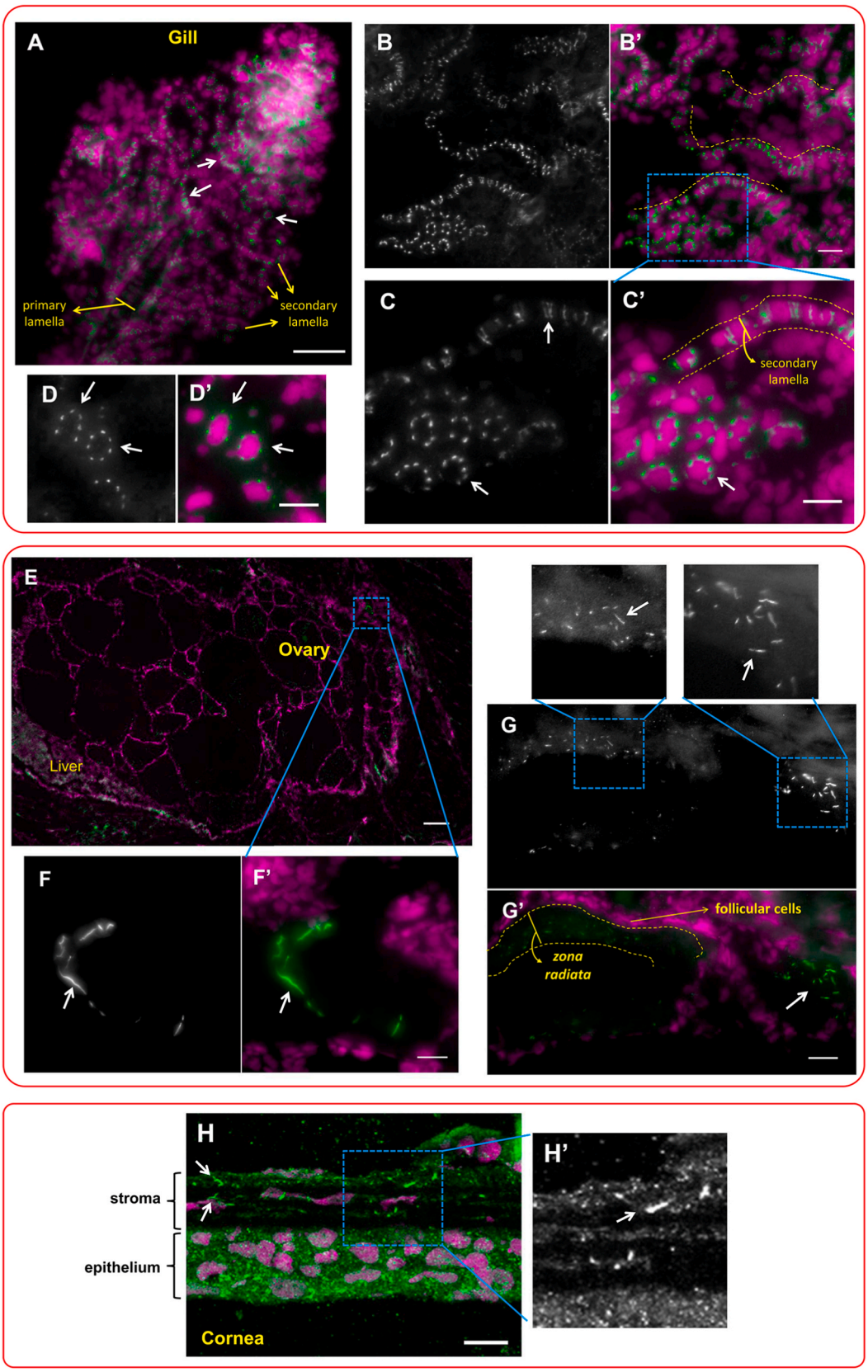

Fig. 5. CTPS cytoophidium in the adult zebrafish. Cryosections of adult zebrafish were probed with *anti*-hCTPS1 antibody (green/gray) and Hoechst (magenta). (A–D) Cytoophidia were observed in secondary lamella of the gills (highlighted by yellow dashed line in B′ and C′). In given cell types, cytoophidia were frequently located around the nucleous (arrows in C and D). (E–G) In the ovary, many cytoophidia were observed in the pre-vitellogenic (F) and vitellogenic follicles (G); cytoophidia are indicated by arrows. (H) In the eye of adult fish, cytoophidia were observed in the stroma layer of the cornea (arrows in H). Scale bars = 50 μm in (E), 20 μm in (A) and (B), and 10 μm in (C), (D), (F), (G) and (H).

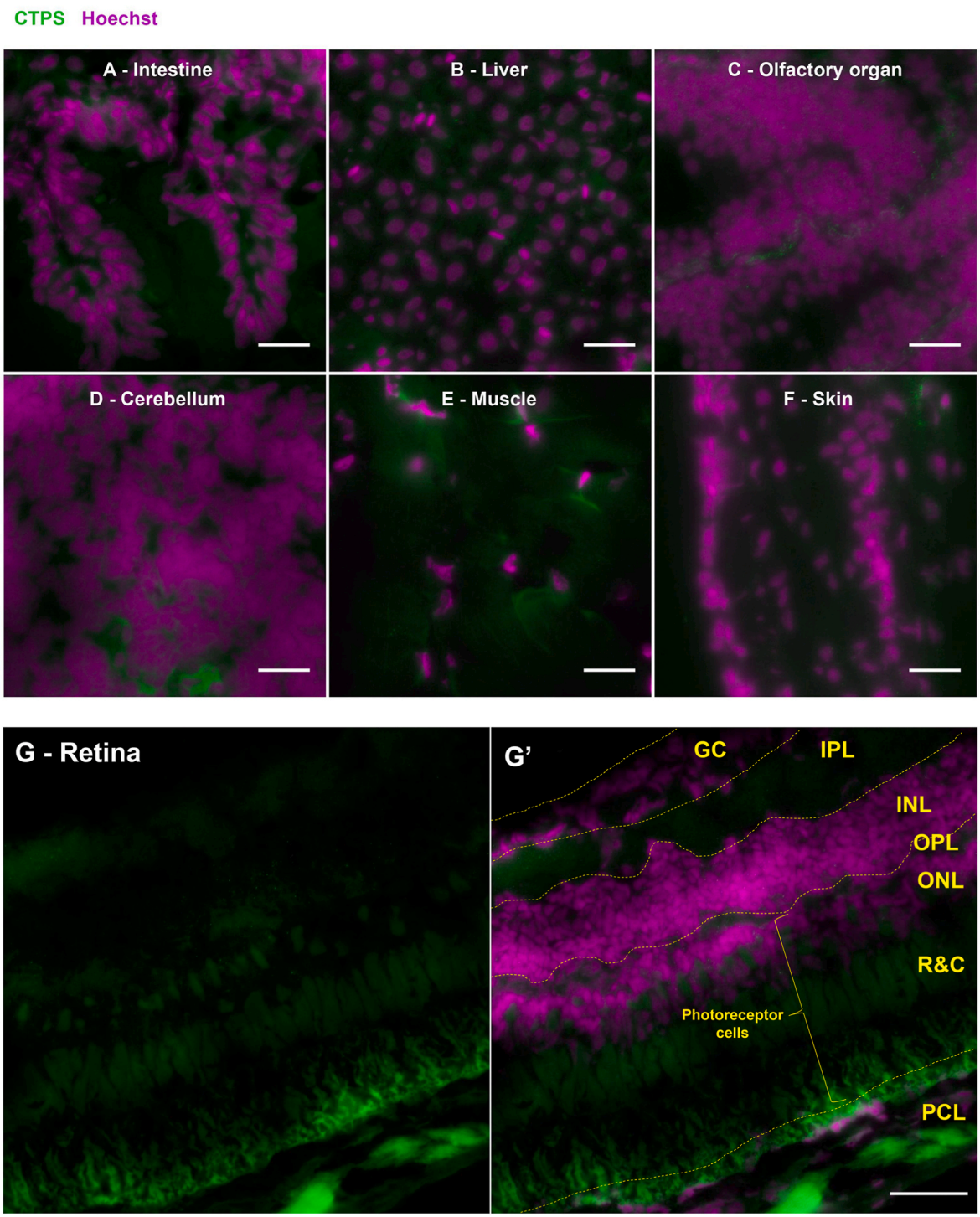

Fig. 6. Tissues of adult zebrafish without the cytoophidium. (A–G) Representative images of adult zebrafish tissues labeled with *anti*-hCTPS1 antibody (shown in green). The selected tissues show no cytoophidia. (G′) Retina layers: GC = ganglion cells, IPL = inner plexiform layer, INL = inner nuclear layer, OPL = outer plexiform layer, ONL = outer nuclear layer, R&C = rods and cones, PCL = pigment cell layer. Scale bars = 10 μm in (A–F) and 20 μm in (G′).

for further research on the function and regulation of the zebrafish CTPS cytoophidium *in vivo*. Furthermore, the finding that supplementing the buffer with DON induces formation of long cytoophidia in the gallbladder and intestine, in which no cytoophidium was detectable without drug treatment, indicates that DON is an effective inducer of zebrafish cytoophidium formation *in vivo*. Taken together, our findings provide basic information on the properties of the zfCTPS cytoophidium, which is particularly valuable for future investigation into the physiological importance of this structure in vertebrates.

3. Materials and methods

3.1. Animals

Zebrafish (*Danio rerio*) AB strain was used throughout this study. Embryos and fish were kept at 28.5 °C for all subsequent assays. Fish experiments were compliant to the general animal welfare guidelines and protocols approved by a legally authorized animal welfare committee: ShanghaiTech University, ShanghaiTech Animal Welfare

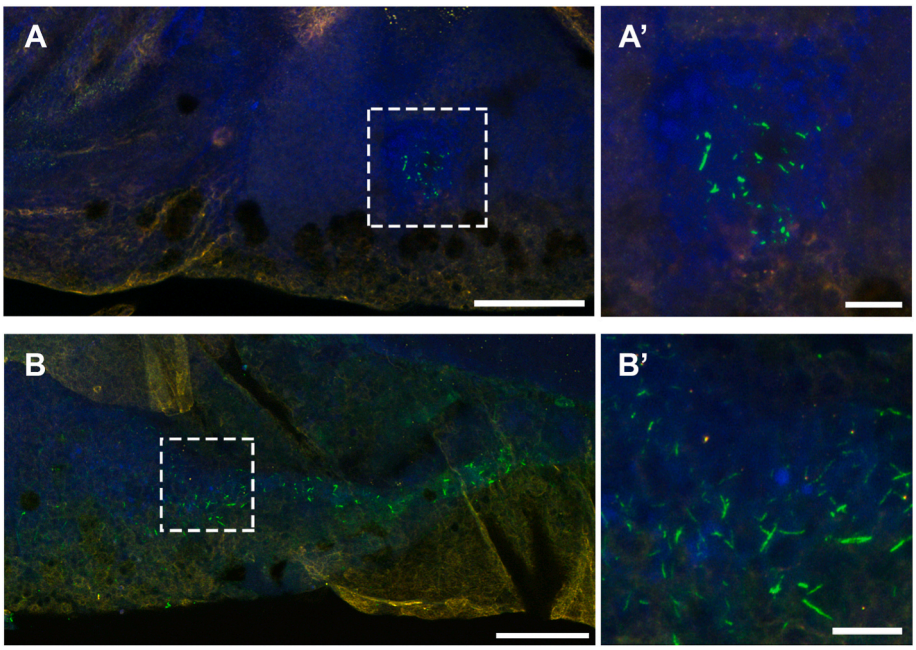

Fig. 7. CTPS cytoophidium in the adult zebrafish. Whole-mount immunofluorescence of 7 dpf larvae treated with DON (10 μg/ml) for 1 day. Signals of *anti*-hCTPS1 antibody shown in green, anti-tubulin antibody shown in red and DAPI shown in blue. (A and B) Representative images of the lateral view of larvae with cytoophidia in the gallbladder (A) and gut (B). (A′ and B′) Magnified images of outlined areas in (A) and (B). Scale bars = 100 μm in (A) and (B), 20 μm in (A′) and (B′).

Committee under the number 20200903003.

3.2. Constructs

Zebrafish CTPS coding sequences for the isoforms 1a and 1b (NCBI Reference Sequence: NM_199211.2; NM_001111247.1) were amplified with primers shown in Table 1 from zebrafish cDNA (see RT-qPCR methods for details) and cloned into the pCMV3 vector (Sino Biological) with tags at the N-terminus (Flag for zfCTPS1a, Myc for zfCTPS1b) with ClonExpress UItra One Step Cloning Kit (C115, Vazyme) according to the manufacturer's protocol. The zfCTPS1a and zfCTPS1b genes without N-terminus tags were fused to mCherry at C-terminus and cloned into a pTol-Hsp70 vector with the same system. Site-directed mutagenesis was carried out by linearizing target constructs with primers containing individual point mutations (Table 1), followed by recirculation of the plasmid with ClonExpress One Step Cloning Kit (C113, Vazyme).

3.3. Cell culture and transfection

Wild-type HEK 293T cells and the hCTPS1-GFP tagged HEK 293T cells were cultured in DMEM with high glucose (Thermo Fisher Scientific) and supplemented with 10% FBS (Thermo Fisher Scientific), 2 mM L-Glutamine and 1% Gibco Antibiotic-Antimycotic (Thermo Fisher Scientific). All cells were cultured in a 37 °C humid incubator with 5% CO2. For cell transfection, TurboFect transfection reagent (R0531, Thermo Fisher Scientific) was used according to instructions provided by the manufacturer. For stimulating cytoophidium assembly, 10 μg/ml DON (D2141, Sigma-Aldrich) and 100 μM DAU (sc-394445, Santa Cruz Biotechnology) were added into the medium as described.

3.4. Immunofluorescence

Immunofluorescence probing on cultured cells was performed as previously described [36]. Immunofluorescence on whole-mount larvae was performed following the published protocol [37]. For cryosection

Table 1
Primers.

Primers used for RT-qPCR (5' -> 3')			
	Target gene	*Forward Primer*	*Reverse Primer*
Primers for zebrafish cDNA	zf-CTPS1a	CCTGCAGAAAGGGTGTCGAT	TTCAGACAGCAGGCCCATTT
	zf-CTPS1b	GTTTTGCCATGTCGAACCCG	AGTGAACCATGCCCTGATCC
	zf-β-Act	CTCTTCCAGCCTTCCTTCCT	GCACTGTGTTGGCATACAGG
	zf-GAPDH	TGCTGGTATTGCTCTCAACG	GCCATCAGGTCACATACACG
	zf-HPRT1	TTGCAGTAGCTTGTCGGTGT	CAGACGTTCAGTTCGGTCCA
	zf- TUBα-1a	TGGTACGTGGGTGAGGGTAT	TCCATTGGTTGTCCAATTTTCAC
Amplification of coding sequences from total zf-cDNA for overexpression (5' -> 3')			
	Forward Primer (blue = N′ tag)	*Reverse Primer*	
Flag-zf-CTPS1a	GACTACAAAGACGATGACGACAAGATGATCAGCAAAATGAAGTATATTCTGG	TTATTCCTGAGCAATTGAACGTAG	
Myc-zf-CTPS1b	GAACAAAAACTCATCTCAGAAGAGGATCTGATGAAGTACATACTGGTGACAGGG	TTAAGAAAGCGATGGGAATTTG	
Primers for zf-CTPS point-mutations (5' -> 3')			
	Forward Primer	*Reverse Primer*	
zf-CTPS1a^{H355A}	CAGGAAGAGCCAGTGAAGTACGCTGAGGCATGGCAGAAGCTCTG	GTACTTCACTGGCTCTTCCTG	
zf-CTPS1b^{H355A}	CAGGATGAGCCAGTGAAGTATGCTGAGGCCTGGCAGAAGCTCTG	TACTTCACTGGCTCATCCTG	

on adult zebrafish, animals were sacrificed and embedded with Tissue-Tek O.C.T. compound (Sakura) immediately and kept in −80 °C. Sections were cut to thickness of 5 μm in lateral view. Sections were fixed with 4% paraformaldehyde for 20 min, followed by blocking with Background Sniper (BS966, Biocare) for 15 min. After washing with PBS, sections were then incubated overnight at 4 °C with primary antibody in 1:300 dilution with staining buffer (PBS supplemented with 0.5% Tween and 1% BSA). After washing three times with PBS, sections were incubated for 2 h at RT with secondary antibody 1:500 dilution in staining buffer with DAPI. After washing three times with PBS, sections were mounted and observed under a fluorescent microscope. Organs and tissues on sections were identified by tissue morphology referring to a published paper [30]. Antibodies used in this study: rabbit polyclonal *anti*-hCTPS1 antibody (15914-1-AP, ProteinTech), mouse *anti*-Myc monoclonal antibody 9E10 (sc-40, Santa Cruz Biotech), mouse anti-Flag antibody (F1804, Sigma-Aldrich), mouse anti-tubulin antibody (MAB1637, Sigma-Aldrich). DyLight 488-conjugated, CyTM3-conjugated and DyLight 649-conjugated donkey polyclonal anti-mouse IgG antibody (715-165-151, 715-485-151, 715-495-151, Jackson ImmunoResearch), CyTM3-conjugated donkey polyclonal anti-rabbit IgG antibody (711-165-152, Jackson ImmunoResearch), Alexa Fluor® 488-conjugated, Alexa Fluor® 647-conjugated donkey polyclonal anti-rabbit IgG antibody (A-21206, A-31573, Invitrogen Mol Probes).

4. RT-qPCR

Adult zebrafish were sacrificed and eye, muscle, intestine, and a mix of organs were collected immediately. The mix of organs contained parts of liver, kidney, pancreas, heart, gills, spleen and perhaps other organs. For the 10 dpf larvae, the entire animal was used. Samples were ground up with a tissue homogenizer and RNA was extracted using TransZol Up Plus RNA Kit (ER501, TransGen Biotech). Reverse transcription was performed with PrimeScrip RT Master Mix (RR036A, Takara). Quantitative PCR (qPCR) was performed with ChamQ Universal SYBR qPCR Master Mix (Q711-02, Vazyme), and the signal was detected by QuantStudio 7 Flex System (Applied Biosystems) following the manufacturer's protocol. Standard 60° Tm annealing temperature and 40 amplification cycles were used for all primer pairs. The quality of reaction was evaluated by melt curves. Target Ct genes were analyzed by comparison of housekeeping references using the ΔΔCt method [38]. First delta was housekeeping geomean. Second delta was larval levels. Housekeeping was a geomean of β-Act, GAPDH, HPRT1 and TUBα-1a. Primers targeting specific zfCTPS isoforms for RT-qPCR were designed using the primer-BLAST NCBI online tool. All primer sequences are listed in Table 1.

4.1. Microscopy and image analysis

Fluorescent images were acquired with a laser-scanning confocal microscope (TCS SP8 STED 3X and TCS SP5 II, Leica) and the fluorescent microscope Axio Imager Z2 or M2 (Zeiss) under 20X and 40X objectives. Images were analyzed with ImageJ software.

5. Statistics

Average Ct values in the RT-qPCR analysis were statistically compared by Mann-Whitney test. Correlations between variables were analyzed by Pearson's R test and the R^2 value is shown. P-value <0.05 was considered statistically significant. Statistical analysis was performed with GraphPad Prism software. Sequence identity alignments were performed with the CLUSTAL Omega (1.2.4) multiple sequence alignment program.

Credit author statement

Chia-Chun Chang: Conceptualization, Methodology, Investigation, Formal analysis, Writing – original draft, Writing – review & editing, Visualization. Gerson Dierley Keppeke: Conceptualization, Methodology, Investigation, Formal analysis, Writing – original draft, Writing – review & editing, Visualization. Christopher L. Antos: Resources. Min Peng: Investigation. Luis Eduardo Coelho Andrade: Supervision. Li-Ying Sung: Supervision. Ji-Long Liu: Conceptualization, Resources, Writing – review & editing, Supervision, Project administration.

Funding

This work was supported by ShanghaiTech University, the UK Medical Research Council (Grant No. MC_UU_12021/3 and MC_U137788471), National Natural Science Foundation of China (Grant No. 31771490) and FAPESP (Fundação de Amparo à Pesquisa do Estado de São Paulo, Grant No. #2017/20745-1). Funding providers had no involvement in the study design, collection, analysis and interpretation of data, writing of the report, and in the decision to submit the article for publication.

Declaration of competing interest

The authors declare no conflicts of interest.

References

[1] J.L. Liu, The cytoophidium and its kind: filamentation and compartmentation of metabolic enzymes, Annu. Rev. Cell Dev. Biol. 32 (2016) 349–372.
[2] C.K. Park, N.C. Horton, Structures, functions, and mechanisms of filament forming enzymes: a renaissance of enzyme filamentation, Biophys. Rev. 11 (2019) 927–994.
[3] S. Zhang, K. Ding, Q.J. Shen, S. Zhao, J.L. Liu, Filamentation of asparagine synthetase in Saccharomyces cerevisiae, PLoS Genet. 14 (2018), e1007737.
[4] C. Noree, K. Begovich, D. Samilo, R. Broyer, E. Monfort, et al., A quantitative screen for metabolic enzyme structures reveals patterns of assembly across the yeast metabolic network, Mol. Biol. Cell 30 (2019) 2721–2736.
[5] B. Zhang, O.Y. Tastan, X. Zhou, C.J. Guo, X. Liu, et al., The proline synthesis enzyme P5CS forms cytoophidia in Drosophila, J. Genet. Genom. 47 (2020) 131–143.
[6] M. Ingerson-Mahar, A. Briegel, J.N. Werner, G.J. Jensen, Z. Gitai, The metabolic enzyme CTP synthase forms cytoskeletal filaments, Nat. Cell Biol. 12 (2010) 739–746.
[7] E.M. Lynch, D.R. Hicks, M. Shepherd, J.A. Endrizzi, A. Maker, et al., Human CTP synthase filament structure reveals the active enzyme conformation, Nat. Struct. Mol. Biol. 24 (2017) 507–514.
[8] E.M. Lynch, J.M. Kollman, Coupled structural transitions enable highly cooperative regulation of human CTPS2 filaments, Nat. Struct. Mol. Biol. 27 (2020) 42–48.
[9] R.M. Barry, A.F. Bitbol, A. Lorestani, E.J. Charles, C.H. Habrian, et al., Large-scale filament formation inhibits the activity of CTP synthetase, Elife. 3 (2014), e03638.
[10] J.L. Liu, Intracellular compartmentation of CTP synthase in Drosophila, J. Genet. Genom. 37 (2010) 281–296.
[11] C. Noree, B.K. Sato, R.M. Broyer, J.E. Wilhelm, Identification of novel filament-forming proteins in Saccharomyces cerevisiae and Drosophila melanogaster, J. Cell Biol. 190 (2010) 541–551.
[12] J. Zhang, L. Hulme, J.L. Liu, Asymmetric inheritance of cytoophidia in Schizosaccharomyces pombe, Biol. Open. 3 (2014) 1092–1097.
[13] C.C. Chang, G.D. Keppeke, L.Y. Sung, J.L. Liu, Interfilament interaction between IMPDH and CTPS cytoophidia, FEBS J. 285 (2018) 3753–3768.
[14] M. Daumann, D. Hickl, D. Zimmer, R.A. DeTar, H.H. Kunz, et al., Characterization of filament-forming CTP synthases from Arabidopsis thaliana, Plant J. 96 (2018) 316–328.
[15] S. Zhou, H. Xiang, J.L. Liu, CTP synthase forms cytoophidia in archaea, J. Genet. Genom. 47 (2020) 213–223.
[16] C. Noree, E. Monfort, A.K. Shiau, J.E. Wilhelm, Common regulatory control of CTP synthase enzyme activity and filament formation, Mol. Biol. Cell. 25 (2014) 2282–2290.
[17] Z. Wu, J.L. Liu, Cytoophidia respond to nutrient stress in Drosophila, Exp. Cell Res. 376 (2019) 159–167.
[18] K.M. Gou, C.C. Chang, Q.J. Shen, L.Y. Sung, J.L. Liu, CTP synthase forms cytoophidia in the cytoplasm and nucleus, Exp. Cell Res. 323 (2014) 242–253.
[19] C.C. Chang, W.C. Lin, L.M. Pai, H.S. Lee, S.C. Wu, et al., Cytoophidium assembly reflects upregulation of IMPDH activity, J. Cell Sci. 128 (2015) 3550–3555.
[20] W.C. Lin, A. Chakraborty, S.C. Huang, P.Y. Wang, Y.J. Hsieh, et al., Histidine-dependent protein methylation is required for compartmentalization of CTP synthase, Cell Rep. 24 (2018) 2733–2745 e2737.

[21] C.C. Chang, Y.M. Jeng, M. Peng, G.D. Keppeke, L.Y. Sung, et al., CTP synthase forms the cytoophidium in human hepatocellular carcinoma, Exp. Cell Res. 361 (2017) 292–299.
[22] G.N. Aughey, S.J. Grice, J.L. Liu, The interplay between myc and CTP synthase in Drosophila, PLoS Genet. 12 (2016), e1005867.
[23] C. Andreadis, L. Hulme, K. Wensley, J.L. Liu, The TOR pathway modulates cytoophidium formation in Schizosaccharomyces pombe, J. Biol. Chem. 294 (2019) 14686–14703.
[24] Z. Sun, J.L. Liu, mTOR-S6K1 pathway mediates cytoophidium assembly, J. Genet. Genom. 46 (2019) 65–74.
[25] E. Martin, N. Palmic, S. Sanquer, C. Lenoir, F. Hauck, et al., CTP synthase 1 deficiency in humans reveals its central role in lymphocyte proliferation, Nature. 510 (2014) 288–292.
[26] N. Dzaki, W. Wahab, A. Azlan, G. Azzam, CTP synthase knockdown during early development distorts the nascent vertebral column and causes fluid retention in multiple tissues in zebrafish, Biochem. Biophys. Res. Commun. 505 (2018) 106–112.
[27] R. Schonherr, M. Klinge, J.M. Rudolph, K. Fita, D. Rehders, et al., Real-time investigation of dynamic protein crystallization in living cells, Struct. Dyn. 2 (2015), 041712.
[28] R. Schonherr, J.M. Rudolph, L. Redecke, Protein crystallization in living cells, Biol. Chem. 399 (2018) 751–772.
[29] C.C. Chang, G.D. Keppeke, L.Y. Sung, J.L. Liu, Interfilament interaction between IMPDH and CTPS cytoophidia, FEBS J. 285 (2018) 3753–3768.
[30] A.L. Menke, J.M. Spitsbergen, A.P. Wolterbeek, R.A. Woutersen, Normal anatomy and histology of the adult zebrafish, Toxicol. Pathol. 39 (2011) 759–775.
[31] K. Chen, J. Zhang, O.Y. Tastan, Z.A. Deussen, M.Y. Siswick, et al., Glutamine analogs promote cytoophidium assembly in human and Drosophila cells, J. Genet. Genom. 38 (2011) 391–402.
[32] J. Zhang, J.L. Liu, Temperature-sensitive cytoophidium assembly in Schizosaccharomyces pombe, J. Genet. Genom. 46 (2019) 423–432.
[33] X. Zhou, C.J. Guo, H.H. Hu, J. Zhong, Q. Sun, et al., Drosophila CTP synthase can form distinct substrate- and product-bound filaments, J. Genet. Genom. 46 (2019) 537–545.
[34] Z. Sun, J.L. Liu, Forming cytoophidia prolongs the half-life of CTP synthase, Cell Discov. 5 (2019) 32.
[35] P. Rombough, Gills are needed for ionoregulation before they are needed for O(2) uptake in developing zebrafish, Danio rerio, J. Exp. Biol. 205 (2002) 1787–1794.
[36] G.D. Keppeke, C.C. Chang, M. Peng, L.Y. Chen, W.C. Lin, et al., IMP/GTP balance modulates cytoophidium assembly and IMPDH activity, Cell Div. 13 (2018) 5.
[37] D. Santos, S.M. Monteiro, A. Luzio, General whole-mount immunohistochemistry of zebrafish (Danio rerio) embryos and larvae protocol, Methods Mol. Biol. 1797 (2018) 365–371.
[38] K.J. Livak, T.D. Schmittgen, Analysis of relative gene expression data using real-time quantitative PCR and the 2(-Delta Delta C(T)) Method, Methods. 25 (2001) 402–408.
[39] Y.L. Li, J.L. Liu, Hypoosmolality impedes cytoophidium integrity during nitrogen starvation, Yeast 38 (2021) 276–289.
[40] Q.Q. Wang, P.A. Zhao, O.Y. Tastan, J.L. Liu, Polarised maintenance of cytoophidia in Drosophila follicle epithelia, Exp. Cell Res. 15 (2021) 112564.